INTERNATIONAL JOURNAL OF PRECISION ENGINEERING AND MANUFACTURING Vol. 17, No. 10, pp. 1401-1412 OCTOBER 2016 / 1401
DOI: 10.1007/s12541-016-0166-x ISSN 2234-7593 (Print) / ISSN 2005-4602 (Online)

Recent Advances in Biological Uses of Traction Force Microscopy

Youngbin Cho[1], Eun Young Park[1], Eunmin Ko[1], Jin-Sung Park[1], and Jennifer H. Shin[1,#]

1 Department of Mechanical Engineering, KAIST, 291 Daehak-ro, Yuseong- gu, Daejeon 34141, South Korea
Corresponding Author / E-mail: j_shin@kaist.ac.kr, TEL: +82-42-350-3232, FAX: +82-42-350-3210

KEYWORDS: Cellular traction, Traction force microscopy, Physiological stimuli, Microenvironment

Cell traction forces (CTF) generated by the actomyosin cytoskeleton onto a substrate or extracellular matrix (ECM) are essential for many biological processes, including developmental morphogenesis, tissue homeostasis, and cancer metastasis. Because the cellular physical properties are closely related to the pathological states of the cells, affected by various physicochemical stimuli from their neighboring cells or surrounding environments, it is crucial to develop a quantitative measure for cellular responses to these external stimuli. Since the pioneering work of Harris et al. in 1980s[1], traction force microscopy (TFM) has been widely used as a standard tool that allows the optical measurement of cellular tractions exerted on 2- and 3-dimensional soft elastic substrates. Recently, there have been many technical advances in conventional TFM to enhance its spatial and temporal resolutions as well as the range of applicability. In this review, we provide a survey on the recent advancement in TFM, especially with a special emphasis on platforms that can externally apply various stimuli such as fluid shear, mechanical tension or compression, biochemical factors, and electric field in a physiologically relevant regime.

Manuscript received: August 24, 2016 / Revised: September 26, 2016 / Accepted: September 26, 2016

NOMENCLATURE

TFM = traction force microscopy
CTF = cell traction force
ECM = extracellular matrix
FAs = focal adhesions
ECs = endothelial cells
EF = electric field
PA = polyacrylamide
τ = shear stress
PDMS = polydimethylsiloxane
HA = hyaluronic acid
PEGDA = poly (ethylene glycol) diacrylate

1. Introduction

For survival and growth, adherent cells would have to attach onto a suitable substrate or extracellular matrix (ECM).[2,3] During this attachment process, cells are known to accumulate internal stress by increasing actomyosin-mediated contractility inside cells,[4,5] which is transmitted to the extracellular substrate through the focal adhesions (FAs).[6] At the FAs, cells develop cellular traction force (CTF) which correlates closely with cellular functions.[7-9] Traction force microscopy (TFM) is an optical technique that can directly measure the traction of cells cultured on the surface of a soft gel material. The basic concept of the TFM was demonstrated in the experimental work by Harris et al. in 1980 where they observed elastic distortion and wrinkling at the surface of a thin polymeric silicone substrate by migrating cells on the surface.[1] Since then, many have been made to enhance the efforts experimental and analytical techniques by developing more suitable gel materials with a good linear elasticity[10-12] and by employing new methodologies for better quantifications of CTF in a higher spatial resolution.[13-16] More recently, a few attempts were made to implement the TFM technique in three dimensional (3D) microenvironment.[17,18]

Cells in our body are exposed to various physicochemical stimuli from their neighboring cells or extracellular microenvironment (Fig. 1). Upon these stimuli, cells respond by changing their phenotypes and altering genes and protein expressions.[19,20] One of the earliest responses is the changes in the shape and motility, which are mediated by altered

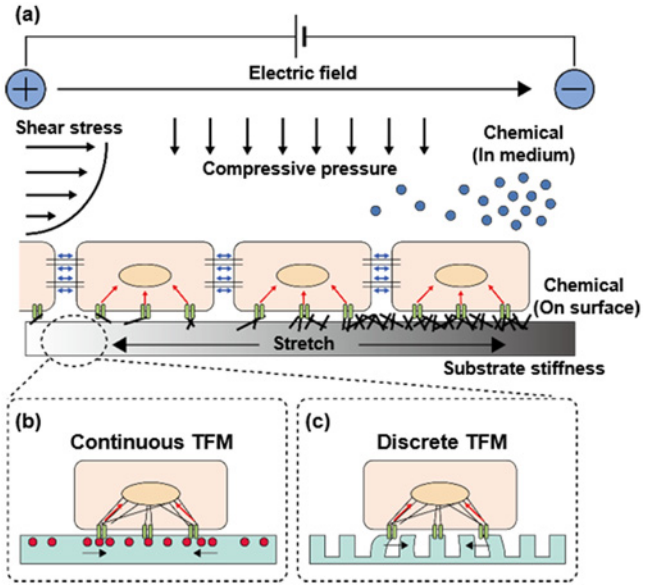

Fig. 1 The schematic descriptions of cells exposed to various physiological stimuli in a ECM environment and CTF measurement. (a) Traction of cells attached on a soft gel matrix is altered by multiple stimuli of mechanical, chemical, and electrical stress. Here, the substrate stiffness and the number of ligand (black bars) to assist the formation of FAs is gradually increased from left (bright color) to right (dark grey color) side. Also, cell-ECM traction and cell-cell tension are each indicated by the red and blue arrows, respectively. (b) The continuous TFM using a soft gel substrate with embedded fluorescent microbeads. (c) The discrete TFM using a microfabricated elastic micropost array.

adhesion characteristics.[21] The adhesion characteristics include the distribution and the strength of the forces by which the cells attach themselves to the substrate.[22] For examples, in response to alteration in hemodynamic shear stress around the bifurcation regions in the vessels, endothelial cells (ECs) change their permeability by remodeling FAs between cell and ECM.[23] Furthermore, acute asthma attack, a clinical syndrome in the airway, is known to arise due to the constricted airways caused by cellular traction generated by airway smooth muscle.[24] Because the physicochemical factors are playing crucial roles in regulating cellular functions, and recent studies pinpoint close correlation between the cellular functions and the CTF, it would be of great interest to investigate the link between the physicochemical stimuli from the surroundings and the alterations in the CTF.

To visualize CTF in a more realistic ECM environment, a number of researchers have established different types of the TFM platforms that integrate various physiological stimuli such as shear flow, stiffness change in the substrates, mechanical stretch, hydrostatic pressure, chemical gradient or electric fields (EFs) (Fig 2). In this review, we provide a detailed description of recent advances in TFM techniques, with a special emphasis on the integrated platforms with the above-mentioned factors (Table 1). In chapter 2, we describe cellular responses onto the fluid shear in a wide physiological range from interstitial flow by extravasation to blood flow in the arterial vascular vessel. Then, we discuss on cellular responses to other mechanical conditions, including a stiffness variation in a substrate, mechanical stretching, and compression by external pressure. The effects of chemical gradients and EFs to CTF are discussed in chapter 3 and chapter 4, respectively. Finally, we summarize our review and discuss some future issues in chapter 5.

2. Measuring CTF with Multiple Mechanical Stimuli

2.1 Microfluidic-based TFM platform with application of a fluid shear

The level of shear stress induced by the blood flow differs largely depending upon the location and pathological conditions. Based on the Poiseuille's law, researchers found out that the ECs experience shear stress between 10 to 70 dyne/cm^2 in the atheroprotective arterial vascular network, 1 to 6 dyne/cm^2 in atherosclerosis-prone sites or in the venous system,[25] and 10^{-4}-10^{-2} dyne/cm^2 in early vessel formation.[26,27] These various ranges of shear stress can be imposed within the microfluidic channel, where the stable fluid flow can be generated during real-time imaging.[28] According to the magnitude of the shear stress, the strategy for flow generation inside the flow channel can be determined. For high shear stress (>10 dyne/cm^2), fluid flow can be easily controlled by either the hydrostatic pressure difference between the inlet and outlet of the channel[29,30] or the peristaltic pump.[31,32] For low shear stress (<4 dyne/cm^2), a syringe pump of different volumes can be utilized to control the flow.[30,33] To quantify the cellular stress changes under the influence of fluid flow, the flow channels can be combined with the covalently bonded hydrogel on a glass coverslip or with the polydimethylsiloxane (PDMS) micropost arrays.

Using these extended TFM platforms, a number of studies have reported the conflicting results on the changes in cell-ECM traction and cell-cell tension under the laminar shear flow of 10 dyne/cm^2. Some studies reported the increase in magnitude of cell-ECM traction and cell-cell tension under shear condition, demonstrated by the enhancement in the cellular traction perpendicular to the flow direction, stress fiber alignment, and the localization of adherens junction proteins at both ends of the stress fibers.[30,32,34,35] In contrast, some other studies showed opposite results. Robert et al. and Conway et al. showed the decrease in magnitude and alignment of cell-ECM traction and cell-cell tension followed by the elongation and alignment of cell body under steady laminar flow.[29,31] They suggested that the flow triggered decrease in total cellular force likely to mediate adherens junction and paracellular gap formation.

Unlike the case of high shear laminar flow, Cecile et al. showed the rapid and more pronounced increase in cell-ECM traction and cell-cell tension under the low shear laminar flow.[33] In addition, Ting et al. and Hur et al. showed that cells had lower traction under the disturbed or oscillatory flow.[30,32]

Until now, whether the increases in cell-ECM traction and cell-cell tension have protective or disruptive roles for vessel maintenance remain controversial, and the underlying mechanisms by which fluid shear stress alters the cellular stresses are still unknown. Therefore, the extended TFM platforms with the integrated stimulator would enable the researchers to investigate the pivotal role of physical stress in the dynamic remodeling of FAs, the cytoskeleton, and cell-cell junctions

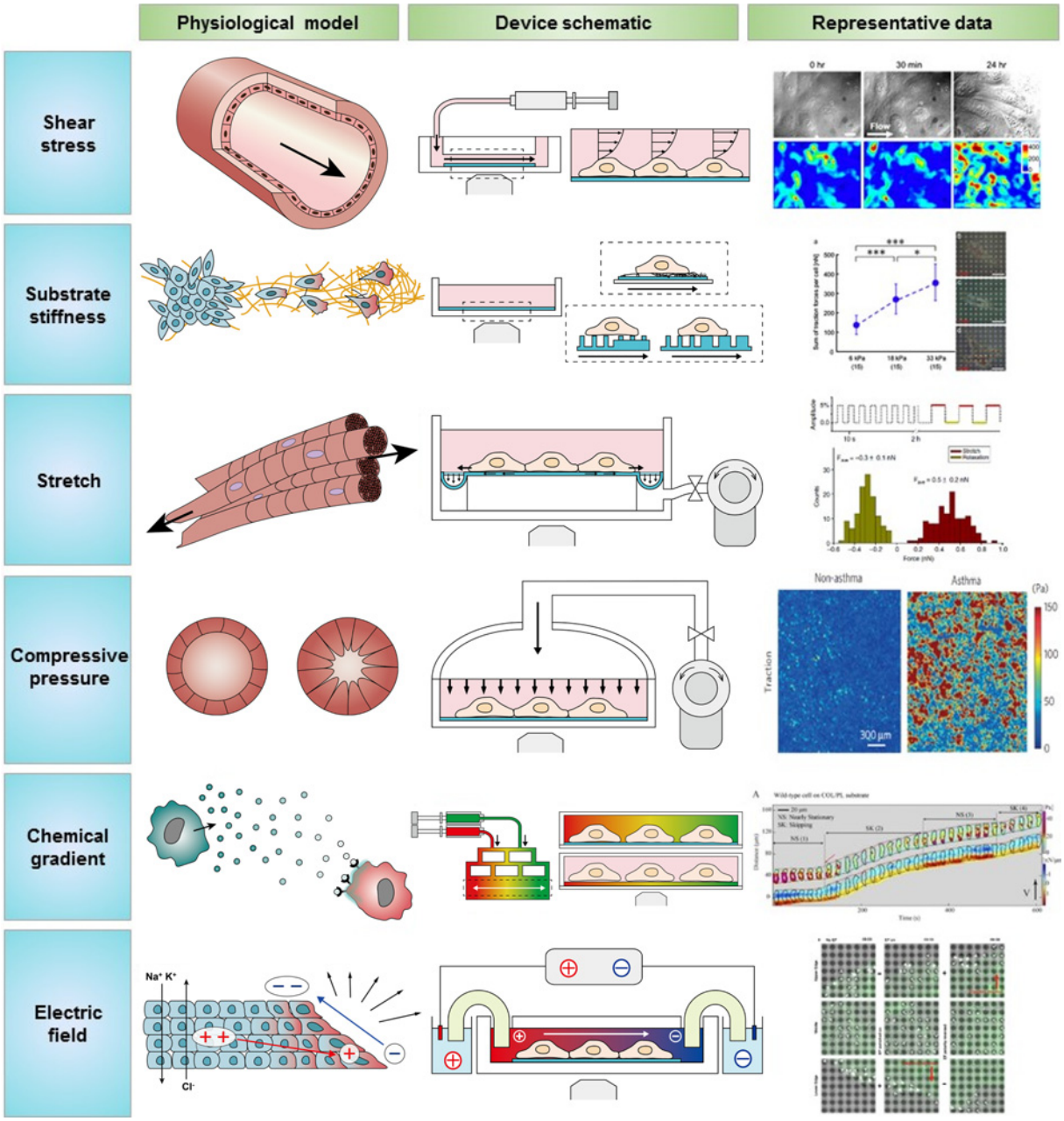

Fig. 2 Different types of the extended TFM platforms combined with physiological stimuli developed to observe the changes in spatiotemporal patterns in CTF. Each physiological and pathological model in different organs or tissues is schematically drawn (first column). Then, the corresponding TFM platforms are schematically described (second column) with representative data set (last column). As shown in second of 1st row, for endothelial cells, they are aligned in CTF as well as their morphology in response to the fluid shear stress (last in the 1st row, reprinted with permission from Hur et al., Proc Natl Acad Sci[30]). The substrate stiffness can be changed by controlling crosslinking rates (upper channel in the middle of 2nd row) or a height and diameter of micropost array (lower channel in middle of 2nd row). According to the previous experiment, CTF becomes increased with a higher value in substrate stiffness (last in 2nd row, reprinted with permission from Maeda et al., J Biomech[58]). When the cells are stretched on a stretchable cell-adhered membrane (second in 3rd row), the alteration in CTF can be induced by cytoskeleton remodeling (last in 3rd row, reprinted with permission from Cui et al., Nat Commun[60]). In airway, epithelial cells experience the higher apical-to-basal compressive stress due to the constriction effect of bronchospasm (second in 4th row). By establishing the compressive pressure on the TFM platform, the simultaneous changes in CTF as well as cell morphology can be induced (last in 4th row, reprinted with permission from Park et al., Nat Mater[76]). Chemical gradients are established by soluble (upper channel) or immobilized factors (lower channel) inside a microfluidic channel combined to the TFM platform. Here, directed cell migration along a spatial gradient of chemoattractant can be induced by altering their CTF (last in 5th row, reprinted with permission from Bastounis et al., J Cell Biol[84]). Lastly, disruption of trans-epithelial potentials induces the generation of EFs at the wound site and induces the direct cell migration toward the wound site (second in 6th row). Here, DC power is applied into the chamber via agar salt bridges to generate EFs through the culture media. At the leading edge of the cell monolayer, they exhibit the different spatiotemporal patterns in their CTF under EFs (last in 6th row, reprinted with permission from Li et al., CMLS[103]).

Table 1 Extended TFM platform

Physiological stimulus		Physiology model	Cell type	Stimulus method	Device Scale	TFM substrate (Continuous, Discrete)	Substrate stiffness	Observation	Ref.
Shear stress		Blood flow	Human umbilical vein endothelial cells (HUVECs) (M*), Human pulmonary artery endothelial cells (HPAECs) (M*)	Syringe or peristaltic pump, Pressure difference between inlet/outlet	Micro-scale	Both available	1.2-1.25 kPa	Shear induces rapid change in alignment of cell-matrix traction and cell-cell tension. Magnitude of stress level is still debatable.	29,30, 31,32, 33,34, 35
Substrate stiffness		Cancer metastasis, Wound healing, Development of nervous system, Stem cell differentiation	Fibroblast (S*), Tenocyte (S*), Human mesenchymal stem cell (hMSC) (S*)	Mixture agent manipulation, Micropost height, diameter	Milli-scale	Both available	0.5-400 kPa 5-80 nN/μm	Cellular traction tends to increase on the stiffer substrate	56,57, 58,59
Stretch		Smooth muscle, endothelial cell dysfunction	Vascular smooth muscle cells (VSMCs) (S*), Primary mouse embryonic fibroblast (S*)	Vacuum in microfluidic chamber	Micro-scale	Both available	2.3 nN/μm	Magnitudes of traction and tension are changed apparent from stiffening and softening of the cells, respectively.	60,62, 65,66, 67
Compressive pressure		Asthma	Primary human bronchial epithelial cells (HBECs) (M*)	Apical-to-basal compressive stress	Milli-scale	Only continuous system reported	1.2 kPa	Pressure induced morphological change is linked with physical stress within collective cells.	76
Cheimcal gradient	**Soluble in medium**	Innate immunity	Neutrophil (S*) Dendritic cell (S*)	Micropipette point source, Microfluidic laminar mixing device	Micro-scale	Both available	1.5-12 kPa	In chemotaxis, traction forces are increased, having a directionality, which is coherent to the directional migration.	85,86, 87,88
	Immobilized on surface	Wound healing	Fibroblast (S*)	Type I collagen density gradient on the surface	Milli-scale	Continuous available, Discrete unavailable	5 kPa	Cells exert higher tractions when the ligand density on substrate is similar to the receptor density.	91,92
Electric field		Wound healing, Cancer metastasis	Madin-Darby canine kidney (MDCK I) (M*)	Agar salt bridges, Steinberg's solution, Ag/Agcl electrodes	Milli-scale	Only discrete system reported	23.2 nN/μm	MDCK I cells at the anode facing edge of the monolayer showed the coordinated, high traction.	103

S*= single cell, M*= multi-cell.

for the proper maintenance of the ECs.

2.2 TFM platform with a variation of substrate stiffness

Substrate stiffness, which varies depending on the types of tissue, is one of the crucial factors that directly influence the cellular stresses. Studies showed that many different types of cells were sensitive to the material property of their microenvironment and respond by altering their intracellular structure through reorganization of FAs[5] and cytoskeleton assembly.[36]

Extensive studies have been devoted to develop strategies for precise control of the substrate stiffness. The very first step would be to select appropriate gel material. First of all, they should be inert biochemically and nontoxic to cells. For proper analysis, these materials must have a linear elastic response to the development of CTF. Transparency would be necessary for microscopic observations. Lastly, the fabrication process should be simple for cell culture.[1,37] In this aspect, several types of gel substrates with distinct material properties have been developed (Table 2). Depending on the range of stresses the cells are generating, different stiffness range would be required. Among different choices, Polyacrylamide (PA) hydrogel and PDMS are the most well-defined materials, separately covering two distinct regimes of low and high stiffness, respectively.

PA gel can be prepared in the low stiffness regime between 0.15 kPa and 100 kPa by altering the ratio of acrylamide and bis-acrylamide. The mechanical properties of the PA substrate show well-controlled linear deformations that are detectable at both macro and micro scale. Along with the ensured linearity until rupture, the PA gel is transparent and can be polymerized in a thin sheet,[5,38] facilitating real-time observation of both fluorescent and phase contrast images simultaneously at high magnifications. These features enable the researchers to track the displacements of the micro beads embedded within the gel surface. Although the PA gel spans over an excellent range of stiffness for

Table 2 Mechanical properties of materials for elastic substrate used in continuous TFM

Material	TFM methods	Dimension	Strengths	Current limitations	Linear-elastic response regime	Stiffness range	Stiffness regulation	Cell type	Ref.
Polyacrylamide (PA) gel	Bead tracking	2D, 2.5D	Architecturally similar to tissue and ECM, No detectable cellular affinity, Hydrophilic, Homogeneous In limited mixture concentration, Transparent, Easy to tune the stiffness, Wide range of elastic modulus, Inert at biochemical change	Additional biofunctionalization is needed, Invisible topographic surface microstructures	Until rupture (*nonlinear response of gel is of a concern)	0.15-100 kPa	Varying the ratio of crosslinking	Superior cervical ganglion neurons Human airway smooth muscle (HASM) cells Swiss 3T3 fibroblast	5,38, 39
Silicone rubber (polydimethyl siloxane, PDMS)	Wrinkling assay, Bead tracking, Pattern deformation	2D	Nontoxic, High refractive index, Biocompatible, Not swelling, Homogeneous, Isotropic	Protein adsorption on substrate surface, Hydrophobicity of surface	~100%	5 -1,720 kPa	Varying the ratio of crosslinking and curing temperature	PTK-1 Fibroblast (human foreskin, cardiac) Keratocyte	15,40
Gelatin	Bead tracking	2D	High sensitivity	Limited to prokaryotes	[gelatin] > 2.5% and temperature < 26°C	2.2-16 kPa	Varying the concentration of gelatin	Dictyostelium	41
Collagen	Bead tracking	2D, 3D	Natural ECM, Homogeneous, Isotropic, Biodegradable	Limited range of linear-elastic regime, PH sensitivity	~5%	~300 Pa	Varying the concentration of collagen and PH	Corneal Fibroblasts	42,43, 44
Hyaluronic acid	Pattern deformation	2D	Natural ECM Can interact with other ECM	Limited range of linear-elastic regime, Rapid degradation	~10%	2-8 kPa	Varying the concentration of mixture	hMSCs 3T3 cell HUVEC cell	45,46, 47,48, 49,50, 51
Modified Polyethylene Glycol Diacrylate (PEGDA)	Bead tracking	3D	Homogeneous, biodegradable	Difficulty in synthesis	Linear in measuring region	~1 kPa	Varying the degree of crosslinking	NIH 3T3 cells	53,54, 55

studying cellular tractions, it may sometimes exhibit nonlinear effects and swell if the gel is not osmotically balanced with the cell culture media.[39] These limitations were shown to be true for other hydrogels and thus the preparation needs to be done with a great care.

PDMS, on the other hand, exhibits better linearity without apparent swelling issues. However, PDMS can be prepared only in the high stiffness range from 100 kPa to 1,800 kPa. The stiffness of PDMS is controlled by changing the ratio of silicone elastomer to curing agent.[40] When less amount of curing agent is used (stiffness values of lower than 100 kPa), the surface of PDMS elastomer appears sticky, showing inconsistent mechanical response probably due to incomplete curing that results in excess uncapped reactive groups on the surface. To avoid these problems, researchers used PDMS as micropost arrays, instead of a flat 2D sheet, so that they could adjust its stiffness by controlling a height and diameter of micropost.[15]

While the majority of traction studies utilize either PA gel or PDMS, other materials have been tested as summarized in Table 2. Gelatin gel is an alternative to PA gel and features multiple advantages including biocompatibility and easiness in synthesis and thickness control. These advantages allow the high spatial and temporal resolution imaging. However, because the stiffness is controlled only by the concentration of gelatin, the stiffness range is narrow, thus limiting its uses for different cell types. So it was specifically used to measure the traction force of fast moving cells like 'Dictyostelium' and for calcium imaging by high-magnification objectives.[41]

Collagen also is another alternative. Because it plays an important role in regeneration process of wound healing as a major ECM components, it offers a great suitability for measuring CTF mimicking such pathological state. More importantly, it could support 3D ECM environment that allows us 3D TFM measurements for cells embedded inside gel due to its small strain in elasticity and bio-degradability.[42,43] Similarly, to the case of gelatin, the range of stiffness for collagen gel is narrow. Fortunately, a few different strategies have been reported to increase the range of its stiffness such as pH change and adding synthetic cross-linkers[44] but there remain compatibility issues with these modifications.

Hyaluronic acid (HA) gel, which has a low stiffness value in a narrow range from 2 kPa to 8 kPa, is a polysaccharide chain with a linear structure, generally found in a soft tissue and synovial fluid *in vivo*. Due to its high biocompatibility,[45-47] HA-based hydrogels are emerging candidates for stem cell culture.[48,49] Nevertheless, the poor mechanical properties of rapid degradation and limited linear-elastic regime still remain as the drawbacks, despite a few studies suggested fabrication methods to overcome those limitations.[50,51]

Poly (ethylene glycol) diacrylate (PEGDA) substrate is also a biocompatible, hydrophilic polymer. Due to its resistance to protein

adsorption and nonspecific cell adhesion without specific surface treatment, it can be utilized for establishing the appropriate surroundings to guide cellular response.[52-54] Biodegradability also enables PEGDA substrate as the candidate for 3D traction force microscopy.[55]

On a stiff substrate, cells spread well by organizing actin stress fibers and FAs while on soft substrate they become round shaped with disorganized cytoskeletal structure.[56,57] TFM revealed that the cell spreading area were strongly correlated with FAs and CTF, indicating the importance of tight link between cell shape and FAs and cellular traction in stiffness sensing.[56,58] Furthermore, substrate stiffness also induces directional migration. Difference in actin stress fiber and FAs on different substrate stiffness induces the cytoskeleton polarization within the cell, which provides the cue for directional migration to the stiff substrate, called durotaxis. Trichet et al. designed a durotaxis assay by changing the diameter of micropost arrays on the same substrate plane.[59] They found that cells tended to move toward the stiff substrate with polarized actin cytoskeleton on the stiff side after sensing the border area between soft and stiff microposts. Stiffness studies indicate that substrate rigidity and response in cytoskeleton critically decide the cellular function such as spreading and migration.

2.3 TFM platform with mechanical stretching

Most types of cells in our body including non-muscle cells as well as muscle cells experience very common stretching and relaxation during the athletics, walking or even breathing motion.[60-62] Stretch induces cellular responses such as growth, differentiation and secretion via mechanotransduction through integrins, mechanically activated channels, cytoskeletons and other junctional proteins.[61,63,64]

In mechanical stretch, generally several parameters can be defined:[63] magnitude of strain, frequency, stretching mode (biaxial, uniaxial, and equiaxial), strain rate, stretch waveform (cyclic, and static), and relaxation portion of cycle. Those stretch parameters are determined for specific experimental objectives such as mimicking disease, inducing differentiation, cell adaptation, or others. There are no specific guidelines for stretch parameters but 1-10% (magnitude of strain) and 0.1-1 Hz (frequency) conditions are commonly used in various studies.[61]

To stretch the cell-adhered substrate while measuring traction force, two types of stimulating methods have been developed: indentation[60,62] and pneumatic deformation.[65-67] In case of indentation method, the upward motion of loading post underneath the membrane to expand the membrane,[60] or downward motion of loading post to bulge out the hydrogel is used to stretch the surface.[62] The pneumatic deformation method applies vacuum within the evacuation chamber to pull the cell-adhered substrate, and the substrate deformation induces stretch on cell.[65,67] For the TFM analysis, hydrogel or micropost arrays are integrated on the stretchable membrane. In the case of the hydrogel, the enhancement of the adhesion between hydrogel-elastomer membrane has been studied for maintaining the stable integrity between two other elastic materials under the transient strain induced by stretch.[68] Commonly, PA gel is used as the hydrogel due to its well-defined large acceptance range of linear elasticity and easiness of stiffness control (Table 2). In the case of the micropost-based TFM, Mann et al. verified that the stiffness of micropost used in cyclic stretch experiment did not change whether they are stretched or not, indicating that the stiffness variation in accordance with stretching can be excluded in well-designed microposts.[67]

In response to the stretching, cells dominantly change their cellular stress by regulating the adhesion and cytoskeletal proteins.[61,65,69] The well-known response is reinforcement of cytoskeletal tensions (stiffening) by increasing FA assembly and actin polymerization.[61] Cui et al. observed that the cyclic stretching induces increased cell-ECM traction of fibroblast with enhanced stress fiber formation, which indicates the cellular stiffening[60]. This stiffening is reversible. Numerous stretch experiments in vascular smooth muscle cells, human airway smooth muscle cells, and A549 human alveolar epithelial cells showed that cell-ECM traction increased soon after stretching, but the recovery to the original physical state or even the loosening were observed during static stretching.[62,66,67] Not only the cell-ECM traction but the cell-cell tension were also changed in collective epithelial cell cluster (Madin-Darby canine kidney cell, MDCK).[65] Such phenomena coincide with the recent studies about the fluidization of cytoskeletons (softening) in response to transient stretch.[69]

2.4 TFM platform with compressive pressure

Asthma, a common clinical syndrome in airway, is closely related to the decline in lung functions attributed by the structural changes termed airway remodeling.[70] Besides the inflammatory effect, it has been studied that apical-to-basal compressive stress induced by constriction effect of bronchospasm triggers morphological responses in chronic asthma.[71] During maximal bronchoconstriction, airway epithelial cells are typically subjected to compressive stress at a magnitude of 30 cm H_2O, which is at least an order of magnitude greater than normal breathing situation.[71]

To establish the compressive pressure model, researchers have set air-liquid interface (ALI) culture platform implemented with transepithelial air-pressure gradient to give compressive stress.[72,73] Recently, as the tissue remodeling has been linked to collective cell jamming and unjamming phenomena,[74,75] Park et al. provided the evidence that cell morphology rearrangement is closely linked with physical adhesive stresses within the collective bronchial epithelial under mechanical compression environment by using TFM.[76] The challenge for stress measurement was that, they had to use the 1.2 kPa polyacrylamide gel substrate instead of the traditional transwell substrate which disabled them from establishing ALI culture environment. Despite of medium fulfilled culture condition instead of ALI environment, they showed the similar cooperative cellular response with the previous ALI environment results under hydrostatic compression.

3. TFM Platform with Chemical Gradient Generating System

Cell-released chemicals such as chemokines, hormones, growth factors, and ECM components exist during embryonic development, cancer metastasis, blood vessel formation and remodeling, tissue regeneration, and immune responses.[77,78] Cells receive the immediate chemical signals from surroundings through specific receptors on their surface, and process the signals to modulate their behaviors such as cell adhesion, alignment, and migration.[77,79,80] Especially a gradient in chemical concentration is one of the directional cues for the cell

migration.[79,81] Such directional migration in response to a chemical can be classified based on where chemical gradient is developed in a soluble fluid or in an immobilized on the ECM, called chemotaxis and haptotaxis, respectively.[77] As several studies have provided the evidence of the relation between migration direction and cell-ECM traction distribution, identifying the cellular force during directional migration under chemical gradient is important.

In soluble factor gradient generation, there are two kinds of methods based on the molecular transportation principles:[82-84] diffusion-based gradient and convection-based gradient. First, the diffusion-based gradient is induced by the chemical concentration differences, where the molecule diffusivity and time are essential factors. This method is easy to form chemical gradient but inappropriate to generate stable and complex gradient shape over time.[83] Therefore, when the TFM is implemented to these techniques, the experiment chamber will be appropriate for measuring cellular traction of fast moving cells for short-term period. Micropipette method is representative example of diffusion-based gradient generation with TFM.[85,86] Convection-based gradient is generated by mixing the chemicals through the microfluidic channel, where flow is introduced by syringe pump.[87-89] This method is suitable for precise control of gradient shape over time and protection from the disturbance affected by external physical factors with CTF measurement,[87-89] but flow induced shear stress effect on the cell is inevitable.[83,84]

For the immobilized chemical gradient formation on the substrate, numerous techniques have been developed:[77,90] chemical deposition, microcontact printing, and microfluidic mixing device. Despite of the extensive studies on the methodological approaches and cell migration in response to an immobilized chemical gradient, traction characterization has been less studied due to the difficulties in scale down, tune and binding.[90] Recently, Jessica et al. developed the gradually collagen-immobilized PA gel by conjugating the ultraviolet (UV)-curable peptides.[90]

In pathological conditions, immune cells are typically directed by the soluble-factor gradient such as chemokines formed from the injured sites or pathogens.[78] During this chemotaxis, immune cells use effective strategies for directional migration. Dendritic cells (DCs) and neutrophils generated higher cell-ECM traction in a gradient of soluble factor rather than treatment of chemicals.[86,87,89] Such increased cell-ECM tractions were maximized when the mean concentration and the steepness are similar to the density of receptors on cell surface in a 200-1,500 receptor/μm^2 range[91] and binding affinity of receptor in a 1-10,000 picomolar range.[91,92] Cells show spatially polarized traction development toward chemoattractant.[86,87,89] Surprisingly, such polarized traction map preceded the migration for few minutes. Taken together, immune cells seemed to manipulate the cell-ECM traction to perform their immunologic roles in innate defense system. Unlike the chemotaxis, traction generation during haptotaxis, directed migration of cells in response to an immobilized gradient on a substrate, is largely unknown. Few studies found that fibroblast exerted higher cell-ECM traction when ECM protein density on the substrate are approximately equal to the integrin density on the cell surface,[91,92] which is similar to the observation in immune cell chemotaxis.[87,89] Thus, the ligand-receptor interaction seems to be significantly participated in the cellular force generation as well as the directed cell migration in response to either soluble or immobilized gradient.

4. TFM Platform with Electric Field Generating System

Direct current electric field (dcEF) are frequently found in living organisms such as at wound (40-180 mV/mm) and tumor metastatic sites, providing a strong directional cue for cell migration (i.e., electrotaxis).[93-95] Among them, in wound healing, the electrotactic migration of epithelial cells is known to play a crucial role in repairing the damage rather than other stimuli *in vivo*.[93] EF induced asymmetric activation of the cell membrane receptors by the ionic gradient is considered to be important for single cell electrotaxis.[93, 96] However, when it comes to electrotaxis in collective cells, it is difficult to understand the precise mechanism of cohesive migration toward electric poles[96] because of the complex physical balance between cell-ECM traction at leader cell toward substrate and tension at cell-cell junction.[97-99] Along with the recent advances in TFM, the investigation to draw physical pictures of electrotaxis in collective cells just began to start.

For several decades, many researchers have established EF-stimulating cell culture chamber *in vitro*, well reviewed in Cortese et al..[100] These chambers are able to apply the EF through the cell culture media in a range from 0.1 V/cm to 10 V/cm, where the voltage is applied via two Ag/AgCl electrodes connected to the Steinberg's solution and two agar salt bridges. Furthermore, as chamber structure critically influence the voltage drop efficiency and the maintenance of medium properties such as pH, temperature and calcium level, it is crucial to establish well-designed EF chamber.[101,102] Optimized EF chambers in several studies show two common features. First, the minimized height of the chamber creates the highest resistance at the cell-stimulation zone, resulting in the concentrated voltage drop following by Ohm's law. Such effective voltage drop lowers the overall system input voltage, reduces the pH change and improves the lifetime of electrodes.[101] Minimized chamber height is also important to lower the temperature rise of the media caused by Joule heating effect,[102] which can cause not only the swelling up of the hydrogel integrated in the chamber but also the disturbance of the cell environment. Second, maximized volume of culture medium in the chamber reservoirs helps to buffer the changes in pH, temperature and calcium level in medium.[102]

Using TFM platform with EF application, Li et al. observed the interesting cell-ECM traction development in a different region within the MDCK I epithelial monolayer.[103] The coordinated, higher traction to the EF was observed on the leader cells at the monolayer edge facing the anode, whereas the opposite edge cells (facing the cathode) or interior cells near the center of the monolayer showed heterogeneous, lower traction.[103] These data seem to indicate the role of anode-facing edge cells in leading the collective migration through enhanced traction.[103] Cohen et al. also observed the independent migration of cells at the edge of monolayer under external EF application, while the interior cells showed highly electrotactic behavior.[101] Taken together, synchronized effect of cell-ECM traction and cell-cell tension within the collective monolayer seems to play an important role in electrotactic collective migration.

5. Challenges and Outlooks

TFM is a novel technique to measure CTF at the interface between cells and elastic two dimensional (2D) substrate or 3D gel matrix. Over the last decade, significant advances in TFM have been achieved to acquire the higher resolution in CTF measurement and combine with other useful techniques to explore unknown phenomena in the field of cell mechanobiology. Here, we summarized detailed descriptions on the recent TFM platforms integrated with external physiological stimuli systems, which have been developed to investigate the phenomena of cell mechanobiology under various physicochemical stimuli. Especially, a traditional TFM platform was successfully embedded into the microfluidic based technique by which CTF can be simultaneously measured under a stable fluid shear in a wide physiological range or a chemical gradient. It still remains a technical challenge for how these TFM platforms integrated with stimuli systems can extend to more physiologically realistic 3D ECM environments. As most of organs *in vivo* consist of multi-cellular clusters, the issue involves the integration of effective methods for generation of 3D cell aggregation with the precise 3D TFM analysis. Further, improvements in TFM technique will contribute significantly to better understanding of cellular sensing and response mechanism to *in vitro* ECM microenvironment, by well reflecting the physical property of ECM and real physiological condition of *in vivo*.

ACKNOWLEDGEMENT

This work was supported by NRF Grant funded by the Korean Government (NRF-2013S1A2A2035518 and 2016K2A9A2A08003761).

REFERENCES

1. Harris, A. K., Wild, P., and Stopak, D., "Silicone Rubber Substrata: A New Wrinkle in the Study of Cell Locomotion," Science, Vol. 208, No. 4440, pp. 177-179, 1980.
2. Chen, C. S., Mrksich, M., Huang, S., Whitesides, G. M., and Ingber, D. E., "Geometric Control of Cell Life and Death," Science, Vol. 276, No. 5317, pp. 1425-1428, 1997.
3. Meredith, J. E., Fazeli, B., and Schwartz, M. A., "The Extracellular Matrix as a Cell Survival Factor," Molecular Biology of the Cell, Vol. 4, No. 9, pp. 953-961, 1993.
4. Murrell, M., Oakes, P. W., Lenz, M., and Gardel, M. L., "Forcing Cells into Shape: The Mechanics of Actomyosin Contractility," Nature Reviews Molecular Cell Biology, Vol. 16, No. 8, pp. 486-498, 2015.
5. Pelham, R. J. and Wang, Y.-l., "Cell Locomotion and Focal Adhesions are Regulated by Substrate Flexibility," Proceedings of the National Academy of Sciences, Vol. 94, No. 25, pp. 13661-13665, 1997.
6. Sheetz, M. P., Felsenfeld, D. P., and Galbraith, C. G., "Cell Migration: Regulation of Force on Extracellular-Matrix-Integrin Complexes," Trends in Cell Biology, Vol. 8, No. 2, pp. 51-54, 1998.
7. Aratyn-Schaus, Y. and Gardel, M. L., "Transient Frictional Slip between Integrin and the ECM in Focal Adhesions Under Myosin II Tension," Current Biology, Vol. 20, No. 13, pp. 1145-1153, 2010.
8. Balaban, N. Q., Schwarz, U. S., Riveline, D., Goichberg, P., Tzur, G., et al., "Force and Focal Adhesion Assembly: A Close Relationship Studied using Elastic Micropatterned Substrates," Nature Cell Biology, Vol. 3, No. 5, pp. 466-472, 2001.
9. Gardel, M. L., Schneider, I. C., Aratyn-Schaus, Y., and Waterman, C. M., "Mechanical Integration of Actin and Adhesion Dynamics in Cell Migration," Annual Review of Cell and Developmental Biology, Vol. 26, No. pp. 315, 2010.
10. Burton, K. and Taylor, D. L., "Traction Forces of Cytokinesis Measured with Optically Modified Elastic Substrata," Nature, Vol. 385, No. 6615, pp. 450-454, 1997.
11. Harris, A. K., Stopak, D., and Wild, P., "Fibroblast Traction as a Mechanism for Collagen Morphogenesis," Nature, Vol. 290, No. 5803, pp. 249-251, 1981.
12. Lee, J., Leonard, M., Oliver, T., Ishihara, A., and Jacobson, K., "Traction Forces Generated by Locomoting Keratocytes," The Journal of Cell Biology, Vol. 127, No. 6, pp. 1957-1964, 1994.
13. Butler, J. P., Tolić-Nørrelykke, I. M., Fabry, B., and Fredberg, J. J., "Traction Fields, Moments, and Strain Energy that Cells Exert on their Surroundings," American Journal of Physiology-Cell Physiology, Vol. 282, No. 3, pp. C595-C605, 2002.
14. Sabass, B., Gardel, M. L., Waterman, C. M., and Schwarz, U. S., "High Resolution Traction Force Microscopy based on Experimental and Computational Advances," Biophysical Journal, Vol. 94, No. 1, pp. 207-220, 2008.
15. Tan, J. L., Tien, J., Pirone, D. M., Gray, D. S., Bhadriraju, K., and Chen, C. S., "Cells Lying on a Bed of Microneedles: An Approach to Isolate Mechanical Force," Proceedings of the National Academy of Sciences, Vol. 100, No. 4, pp. 1484-1489, 2003.
16. Tolić-Nørrelykke, I. M., Butler, J. P., Chen, J., and Wang, N., "Spatial and Temporal Traction Response in Human Airway Smooth Muscle Cells," American Journal of Physiology-Cell Physiology, Vol. 283, No. 4, pp. C1254-C1266, 2002.
17. Franck, C., Hong, S., Maskarinec, S. A., Tirrell, D. A., and Ravichandran, G., "Three-Dimensional Full-Field Measurements of Large Deformations in Soft Materials using Confocal Microscopy and Digital Volume Correlation," Experimental Mechanics, Vol. 47, No. 3, pp. 427-438, 2007.
18. Legant, W. R., Miller, J. S., Blakely, B. L., Cohen, D. M., Genin, G. M., and Chen, C. S., "Measurement of Mechanical Tractions Exerted by Cells in Three-Dimensional Matrices," Nature Methods, Vol. 7, No. 12, pp. 969-971, 2010.
19. Jin, S., Kim, J. H., and Yun, W.-S., "Development of Dynamic Well Plate System for Cell Culture with Mechanical Stimulus of Shear

Stress And Magnetic Field," Int. J. Precis. Eng. Manuf., Vol. 16, No. 10, pp. 2235-2239, 2015.

20. Jo, H. and Shin, J. H., "Special Issue on Mechanobiology and Diseases, Biomedical Engineering Letters, Vol. 5, No. 3, pp. 159-161, 2015.
21. Geiger, B., Spatz, J. P., and Bershadsky, A. D., "Environmental Sensing through Focal Adhesions," Nature Reviews Molecular Cell Biology, Vol. 10, No. 1, pp. 21-33, 2009.
22. McCain, M. L., Lee, H., Aratyn-Schaus, Y., Kléber, A. G., and Parker, K. K., "Cooperative Coupling of Cell-Matrix and Cell–Cell Adhesions in Cardiac Muscle," Proceedings of the National Academy of Sciences, Vol. 109, No. 25, pp. 9881-9886, 2012.
23. Davies, P. F., "Flow-Mediated Endothelial Mechanotransduction," Physiological Reviews, Vol. 75, No. 3, pp. 519-560, 1995.
24. Park, C. Y., Zhou, E. H., Tambe, D., Chen, B., Lavoie, T., et al., "High-Throughput Screening for Modulators of Cellular Contractile Force," Integrative Biology, Vol. 7, No. 10, pp. 1318-1324, 2015.
25. Malek, A. M., Alper, S. L., and Izumo, S., "Hemodynamic Shear Stress and Its Role in Atherosclerosis," JAMA, Vol. 282, No. 21, pp. 2035-2042, 1999.
26. Park, J. Y., White, J. B., Walker, N., Kuo, C.-H., Cha, W., et al., "Responses of Endothelial Cells to Extremely Slow Flows," Biomicrofluidics, Vol. 5, No. 2, Paper No. 22211, 2011.
27. Song, J. W. and Munn, L. L., "Fluid Forces Control Endothelial Sprouting," Proceedings of the National Academy of Sciences, Vol. 108, No. 37, pp. 15342-15347, 2011.
28. Ng, J., Shin, Y., and Chung, S., "Microfluidic Platforms for the Study of Cancer Metastasis, Biomedical Engineering Letters, Vol. 2, No. 2, pp. 72-77, 2012.
29. Conway, D. E., Breckenridge, M. T., Hinde, E., Gratton, E., Chen, C. S., and Schwartz, M. A., "Fluid Shear Stress on Endothelial Cells Modulates Mechanical Tension Across VE-Cadherin and PECAM-1," Current Biology, Vol. 23, No. 11, pp. 1024-1030, 2013.
30. Hur, S. S., Del Alamo, J. C., Park, J. S., Li, Y.-S., Nguyen, H. A., et al., "Roles of Cell Confluency and Fluid Shear in 3-Dimensional Intracellular Forces in Endothelial Cells," Proceedings of the National Academy of Sciences, Vol. 109, No. 28, pp. 11110-11115, 2012.
31. Steward, R., Tambe, D., Hardin, C. C., Krishnan, R., and Fredberg, J. J., "Fluid Shear, Intercellular Stress, and Endothelial Cell Alignment," American Journal of Physiology-Cell Physiology, Vol. 308, No. 8, pp. C657-C664, 2015.
32. Ting, L. H., Jahn, J. R., Jung, J. I., Shuman, B. R., Feghhi, S., et al., "Flow Mechanotransduction Regulates Traction Forces, Intercellular Forces, and Adherens Junctions," American Journal of Physiology-Heart and Circulatory Physiology, Vol. 302, No. 11, pp. H2220-H2229, 2012.
33. Perrault, C. M., Brugues, A., Bazellieres, E., Ricco, P., Lacroix, D., and Trepat, X., "Traction Forces of Endothelial Cells under Slow Shear Flow," Biophysical Journal, Vol. 109, No. 8, pp. 1533-1536, 2015.
34. Lam, R. H., Sun, Y., Chen, W., and Fu, J., "Elastomeric Microposts Integrated into Microfluidics for Flow-Mediated Endothelial Mechanotransduction Analysis," Lab on a Chip, Vol. 12, No. 10, pp. 1865-1873, 2012.
35. Shiu, Y.-T., Li, S., Marganski, W. A., Usami, S., Schwartz, M. A., et al., "Rho Mediates the Shear-Enhancement of Endothelial Cell Migration and Traction Force Generation," Biophysical Journal, Vol. 86, No. 4, pp. 2558-2565, 2004.
36. Discher, D. E., Janmey, P., and Wang, Y.-l., "Tissue Cells Feel and Respond to the Stiffness of their Substrate," Science, Vol. 310, No. 5751, pp. 1139-1143, 2005.
37. Palchesko, R. N., Zhang, L., Sun, Y., and Feinberg, A. W., "Development of Polydimethylsiloxane Substrates with Tunable Elastic Modulus to Study Cell Mechanobiology in Muscle and Nerve," PLoS One, Vol. 7, No. 12, Paper No. e51499, 2012.
38. Dembo, M. and Wang, Y.-L., "Stresses at the Cell-to-Substrate Interface during Locomotion of Fibroblasts," Biophysical Journal, Vol. 76, No. 4, pp. 2307-2316, 1999.
39. Style, R. W., Boltyanskiy, R., German, G. K., Hyland, C., MacMinn, C.W., et al., "Traction Force Microscopy in Physics and Biology," Soft Matter, Vol. 10, No. 23, pp. 4047-4055, 2014.
40. Schwarz, U. S., Balaban, N. Q., Riveline, D., Bershadsky, A., Geiger, B., and Safran, S., "Calculation of Forces at Focal Adhesions from Elastic Substrate Data: The Effect of Localized Force and the Need for Regularization," Biophysical Journal, Vol. 83, No. 3, pp. 1380-1394, 2002.
41. Doyle, A. D. and Lee, J., "Simultaneous, Real-Time Imaging of Intracellular Calcium and Cellular Traction Force Production," Biotechniques, Vol. 33, No. 2, pp. 358-365, 2002.
42. Roy, P., Petroll, W. M., Cavanagh, H. D., Chuong, C. J., and Jester, J. V., "An in Vitro Force Measurement Assay to Study the Early Mechanical Interaction between Corneal Fibroblasts and Collagen Matrix," Experimental Cell Research, Vol. 232, No. 1, pp. 106-117, 1997.
43. Koch, T. M., Münster, S., Bonakdar, N., Butler, J. P., and Fabry, B., "3D Traction Forces in Cancer Cell Invasion," PLoS One, Vol. 7, No. 3, Paper No. e33476, 2012.
44. Da Cunha, C. B., Klumpers, D. D., Li, W. A., Koshy, S. T., Weaver, J. C., et al., "Influence of the Stiffness of Three-Dimensional Alginate/Collagen-I Interpenetrating Networks on Fibroblast Biology," Biomaterials, Vol. 35, No. 32, pp. 8927-8936, 2014.
45. Shu, X. Z., Liu, Y., Palumbo, F. S., Luo, Y., and Prestwich, G. D., "In Situ Crosslinkable Hyaluronan Hydrogels for Tissue Engineering," Biomaterials, Vol. 25, No. 7, pp. 1339-1348, 2004.
46. Baier Leach, J., Bivens, K. A., Patrick Jr, C. W., and Schmidt, C. E.,

"Photocrosslinked Hyaluronic Acid Hydrogels: Natural, Biodegradable Tissue Engineering Scaffolds," Biotechnology and Bioengineering, Vol. 82, No. 5, pp. 578-589, 2003.

47. Park, Y. D., Tirelli, N., and Hubbell, J. A., "Photopolymerized Hyaluronic Acid-based Hydrogels and Interpenetrating Networks," Biomaterials, Vol. 24, No. 6, pp. 893-900, 2003.
48. Gerecht, S., Burdick, J. A., Ferreira, L. S., Townsend, S. A., Langer, R., and Vunjak-Novakovic, G., "Hyaluronic Acid Hydrogel for Controlled Self-Renewal and Differentiation of Human Embryonic Stem Cells," Proceedings of the National Academy of Sciences, Vol. 104, No. 27, pp. 11298-11303, 2007.
49. Chung, C. and Burdick, J. A., "Influence of Three-Dimensional Hyaluronic Acid Microenvironments on Mesenchymal Stem Cell Chondrogenesis," Tissue Engineering Part A, Vol. 15, No. 2, pp. 243-254, 2008.
50. Burdick, J. A., Chung, C., Jia, X., Randolph, M. A., and Langer, R., "Controlled Degradation and Mechanical Behavior of Photopolymerized Hyaluronic Acid Networks," Biomacromolecules, Vol. 6, No. 1, pp. 386-391, 2005.
51. Schanté, C. E., Zuber, G., Herlin, C., and Vandamme, T. F., "Chemical Modifications of Hyaluronic Acid for the Synthesis of Derivatives for a Broad Range of Biomedical Applications," Carbohydrate Polymers, Vol. 85, No. 3, pp. 469-489, 2011.
52. Hahn, M. S., McHale, M. K., Wang, E., Schmedlen, R. H., and West, J. L., "Physiologic Pulsatile Flow Bioreactor Conditioning of Poly (Ethylene Glycol)-based Tissue Engineered Vascular Grafts," Annals of Biomedical Engineering, Vol. 35, No. 2, pp. 190-200, 2007.
53. Hahn, M. S., Miller, J. S., and West, J. L., "Laser Scanning Lithography for Surface Micropatterning on Hydrogels," Advanced Materials, Vol. 17, No. 24, pp. 2939-2942, 2005.
54. Choi, J. H., Jin, H. K., Bae, J.-S., Park, C. W., Cheong, I. W., and Kim, G. M., Fabrication of Detachable Hydrogel Microplates for Separably Patterned Cell Culture, Int. J. Precis. Eng. Manuf., Vol. 15, No. 5, pp. 945-948, 2014.
55. Gobin, A. S. and West, J. L., "Cell Migration through Defined, Synthetic ECM Analogs," The FASEB Journal, Vol. 16, No. 7, pp. 751-753, 2002.
56. Fu, J., Wang, Y.-K., Yang, M. T., Desai, R. A., Yu, X., et al., "Mechanical Regulation of Cell Function with Geometrically Modulated Elastomeric Substrates," Nature Methods, Vol. 7, No. 9, pp. 733-736, 2010.
57. Lo, C.-M., Wang, H.-B., Dembo, M., and Wang, Y.-l., "Cell Movement is Guided by the Rigidity of the Substrate," Biophysical Journal, Vol. 79, No. 1, pp. 144-152, 2000.
58. Maeda, E., Sugimoto, M., and Ohashi, T., "Cytoskeletal Tension Modulates MMP-1 Gene Expression from Tenocytes on Micropillar Substrates," Journal of Biomechanics, Vol. 46, No. 5, pp. 991-997, 2013.
59. Trichet, L., Le Digabel, J., Hawkins, R. J., Vedula, S. R. K., Gupta, M., et al., "Evidence of a Large-Scale Mechanosensing Mechanism for Cellular Adaptation to Substrate Stiffness," Proceedings of the National Academy of Sciences, Vol. 109, No. 18, pp. 6933-6938, 2012.
60. Cui, Y., Hameed, F. M., Yang, B., Lee, K., Pan, C. Q., et al., "Cyclic Stretching of Soft Substrates Induces Spreading and Growth," Nature Communications, Vol. 6, Paper No. 6333, 2015.
61. Wang, J. H.-C. and Thampatty, B. P., "An Introductory Review of Cell Mechanobiology," Biomechanics and Modeling in Mechanobiology, Vol. 5, No. 1, pp. 1-16, 2006.
62. Krishnan, R., Park, C. Y., Lin, Y.-C., Mead, J., Jaspers, R. T., et al., "Reinforcement Versus Fluidization in Cytoskeletal Mechanoresponsiveness," PLoS One, Vol. 4, No. 5, Paper No. e5486, 2009.
63. Riehl, B. D., Park, J.-H., Kwon, I. K., and Lim, J. Y., "Mechanical Stretching for Tissue Engineering: Two-Dimensional and Three-Dimensional Constructs," Tissue Engineering Part B: Reviews, Vol. 18, No. 4, pp. 288-300, 2012.
64. Lee, H.-Y., Bae, J.-H., and Chang, S.-H., "Mechano-Regulation Theory-based Finite Element Analysis on the Effects of Driving Strain History on Cellular Differentiation, Int. J. Precis. Eng. Manuf., Vol. 16, No. 8, pp. 1851-1858, 2015.
65. Casares, L., Vincent, R., Zalvidea, D., Campillo, N., Navajas, D., et al., "Hydraulic Fracture during Epithelial Stretching," Nature Materials, Vol. 14, No. 3, pp. 343-351, 2015.
66. Gavara, N., Roca-Cusachs, P., Sunyer, R., Farré, R., and Navajas, D., "Mapping Cell-Matrix Stresses during Stretch Reveals Inelastic Reorganization of the Cytoskeleton," Biophysical Journal, Vol. 95, No. 1, pp. 464-471, 2008.
67. Mann, J. M., Lam, R. H., Weng, S., Sun, Y., and Fu, J., "A Silicone-based Stretchable Micropost Array Membrane for Monitoring Live-Cell Subcellular Cytoskeletal Response," Lab on a Chip, Vol. 12, No. 4, pp. 731-740, 2012.
68. Tang, J., Li, J., Vlassak, J. J., and Suo, Z., "Adhesion between Highly Stretchable Materials," Soft Matter, Vol. 12, No. 4, pp. 1093-1099, 2016.
69. Trepat, X., Deng, L., An, S. S., Navajas, D., Tschumperlin, D. J., et al., "Universal Physical Responses to Stretch in the Living Cell," Nature, Vol. 447, No. 7144, pp. 592-595, 2007.
70. Park, J.-A., Fredberg, J. J., and Drazen, J. M., "Putting the Squeeze on Airway Epithelia," Physiology, Vol. 30, No. 4, pp. 293-303, 2015.
71. Tschumperlin, D. J., Dai, G., Maly, I. V., Kikuchi, T., Laiho, L. H., et al., "Mechanotransduction through Growth-Factor Shedding into the Extracellular Space," Nature, Vol. 429, No. 6987, pp. 83-86, 2004.
72. Ressler, B., Lee, R. T., Randell, S. H., Drazen, J. M., and Kamm, R.

D., "Molecular Responses of Rat Tracheal Epithelial Cells to Transmembrane Pressure," American Journal of Physiology-Lung Cellular and Molecular Physiology, Vol. 278, No. 6, pp. L1264-L1272, 2000.

73. Tschumperlin, D. J., Shively, J. D., Swartz, M. A., Silverman, E. S., Haley, K. J., et al., "Bronchial Epithelial Compression Regulates MAP Kinase Signaling and HB-EGF-like Growth Factor Expression," American Journal of Physiology-Lung Cellular and Molecular Physiology, Vol. 282, No. 5, pp. L904-L911, 2002.

74. Sadati, M., Nourhani, A., Fredberg, J. J., and Taheri Qazvini, N., "Glass-like Dynamics in the Cell and in Cellular Collectives," Wiley Interdisciplinary Reviews: Systems Biology and Medicine, Vol. 6, No. 2, pp. 137-149, 2014.

75. Sadati, M., Qazvini, N. T., Krishnan, R., Park, C. Y., and Fredberg, J. J., "Collective Migration and Cell Jamming," Differentiation, Vol. 86, No. 3, pp. 121-125, 2013.

76. Park, J.-A., Kim, J. H., Bi, D., Mitchel, J. A., Qazvini, N. T., et al., "Unjamming and Cell Shape in the Asthmatic Airway Epithelium," Nature Materials, Vol. 14, No. 10, pp. 1040-1048, 2015.

77. Wu, J., Mao, Z., Tan, H., Han, L., Ren, T., and Gao, C., "Gradient Biomaterials and their Influences on Cell Migration," Interface Focus, Vol. 2, No. 3, pp. 337-355, 2012.

78. Rot, A. and von Andrian, U. H., "Chemokines in Innate and Adaptive Host Defense: Basic Chemokinese Grammar for Immune Cells," Annual Review of Immunology, Vol. 22, pp. 891-928, 2004.

79. Devreotes, P. and Janetopoulos, C., "Eukaryotic Chemotaxis: Distinctions between Directional Sensing and Polarization," Journal of Biological Chemistry, Vol. 278, No. 23, pp. 20445-20448, 2003.

80. Kim, M., Gweon, B., Koh, U., Cho, Y., Shin, D. W., et al., Matrix Stiffness Induces Epithelial Mesenchymal Transition Phenotypes of Human Epidermal Keratinocytes on Collagen Coated Two Dimensional Cell Culture, Biomedical Engineering Letters, Vol. 5, No. 3, pp. 194-202, 2015.

81. Rodriguez, L. L. and Schneider, I. C., "Directed Cell Migration in Multi-Cue Environments," Integrative Biology, Vol. 5, No. 11, pp. 1306-1323, 2013.

82. Swartz, M. A. and Fleury, M. E., "Interstitial Flow and Its Effects in Soft Tissues," Annual Review of Biomedical Engineering, Vol. 9, pp. 229-256, 2007.

83. Li, J. and Lin, F., "Microfluidic Devices for Studying Chemotaxis and Electrotaxis," Trends in Cell Biology, Vol. 21, No. 8, pp. 489-497, 2011.

84. Somaweera, H., Ibraguimov, A., and Pappas, D., "A Review of Chemical Gradient Systems for Cell Analysis," Analytica chimica acta, Vol. 907, pp. 7-17, 2016.

85. Bastounis, E., Meili, R., Álvarez-González, B., Francois, J., del Álamo, J. C., et al., "Both Contractile Axial and Lateral Traction Force Dynamics Drive Amoeboid Cell Motility," The Journal of Cell Biology, Vol. 204, No. 6, pp. 1045-1061, 2014.

86. Smith, L. A., Aranda-Espinoza, H., Haun, J. B., Dembo, M., and Hammer, D. A., "Neutrophil Traction Stresses are Concentrated in the Uropod during Migration," Biophysical Journal, Vol. 92, No. 7, pp. L58-L60, 2007.

87. Jannat, R. A., Dembo, M., and Hammer, D. A., "Traction Forces of Neutrophils Migrating on Compliant Substrates," Biophysical Journal, Vol. 101, No. 3, pp. 575-584, 2011.

88. Jannat, R. A., Robbins, G. P., Ricart, B. G., Dembo, M., and Hammer, D. A., "Neutrophil Adhesion and Chemotaxis Depend on Substrate Mechanics," Journal of Physics: Condensed Matter, Vol. 22, No. 19, Paper No. 194117, 2010.

89. Ricart, B. G., Yang, M. T., Hunter, C. A., Chen, C. S., and Hammer, D. A., "Measuring Traction Forces of Motile Dendritic Cells on Micropost Arrays," Biophysical Journal, Vol. 101, No. 11, pp. 2620-2628, 2011.

90. Wen, J. H., Choi, O., Taylor-Weiner, H., Fuhrmann, A., Karpiak, J. V., et al., "Haptotaxis is Cell Type Specific and Limited by Substrate Adhesiveness," Cellular and Molecular Bioengineering, Vol. 8, No. 4, pp. 530-542, 2015.

91. Gaudet, C., Marganski, W. A., Kim, S., Brown, C. T., Gunderia, V., et al., "Influence of Type I Collagen Surface Density on Fibroblast Spreading, Motility, and Contractility," Biophysical Journal, Vol. 85, No. 5, pp. 3329-3335, 2003.

92. Rajagopalan, P., Marganski, W. A., Brown, X. Q., and Wong, J. Y., "Direct Comparison of the Spread Area, Contractility, and Migration of Balb/C 3T3 Fibroblasts Adhered to Fibronectin-and RGD-Modified Substrata," Biophysical journal, Vol. 87, No. 4, pp. 2818-2827, 2004.

93. McCaig, C. D., Rajnicek, A. M., Song, B., and Zhao, M., "Controlling Cell Behavior Electrically: Current Views and Future Potential," Physiological Reviews, Vol. 85, No. 3, pp. 943-978, 2005.

94. Nakajima, K.-I., Zhu, K., Sun, Y.-H., Hegyi, B., Zeng, Q., et al., "KCNJ15/KIR4.2 Couples with Polyamines to Sense Weak Extracellular Electric Fields in Galvanotaxis," Nature Communications, Vol. 6, Article No. 8532, DOI No. 10.1038/ncomms9532, 2015.

95. Zhao, M., "Electrical Fields In Wound Healing-An Overriding Signal that Directs Cell Migration," Seminars in Cell & Developmental Biology, Vol. 20, No. 6, pp. 674-682, 2009.

96. Haeger, A., Wolf, K., Zegers, M. M., and Friedl, P., "Collective Cell Migration: Guidance Principles and Hierarchies," Trends in Cell Biology, Vol. 25, No. 9, pp. 556-566, 2015.

97. Trepat, X., Wasserman, M. R., Angelini, T. E., Millet, E., Weitz, D. A., et al., "Physical Forces during Collective Cell Migration," Nature Physics, Vol. 5, No. 6, pp. 426-430, 2009.

98. Kim, J. H., Serra-Picamal, X., Tambe, D. T., Zhou, E. H., Park, C.

Y., et al., "Propulsion and Navigation within the Advancing Monolayer Sheet," Nature Materials, Vol. 12, No. 9, pp. 856-863, 2013.

99. Tambe, D. T., Hardin, C. C., Angelini, T. E., Rajendran, K., Park, C. Y., et al., "Collective Cell Guidance by Cooperative Intercellular Forces," Nature Materials, Vol. 10, No. 6, pp. 469-475, 2011.

100. Cortese, B., Palamà, I. E., D'Amone, S., and Gigli, G., "Influence of Electrotaxis on Cell Behaviour," Integrative Biology, Vol. 6, No. 9, pp. 817-830, 2014.

101. Cohen, D. J., Nelson, W. J., and Maharbiz, M. M., "Galvanotactic Control of Collective Cell Migration in Epithelial Monolayers," Nature Materials, Vol. 13, No. 4, pp. 409-417, 2014.

102. Song, B., Gu, Y., Pu, J., Reid, B., Zhao, Z., and Zhao, M., "Application of Direct Current Electric Fields to Cells and Tissues in vitro and Modulation of Wound Electric Field in Vivo," Nature Protocols, Vol. 2, No. 6, pp. 1479-1489, 2007.

103. Li, L., Hartley, R., Reiss, B., Sun, Y., Pu, J., et al., "E-Cadherin Plays an Essential Role in Collective Directional Migration of Large Epithelial Sheets," Cellular and Molecular Life Sciences, Vol. 69, No. 16, pp. 2779-2789, 2012.